

On the Influence of Elastic Deformation for Residual Stress Determination by Sharp Indentation Testing

Per-Lennart Larsson

(Submitted March 17, 2017; in revised form June 16, 2017; published online July 6, 2017)

The determination of residual stresses in engineering materials using sharp indentation testing is studied analytically and numerically. The numerical part of the investigation is based on the finite element method. In particular, the effect from elastic deformations on global indentation properties is discussed in detail. This effect is essential when residual stresses are to be determined based on the change of the contact area due to such stresses. However, standard relations for this purpose are founded on the fact that the material hardness is invariant as regards residual (applied) stresses. Presently, this assumption is scrutinized and it is shown that it is only valid at dominating plastic deformation around the contact region. The hardness dependence of residual stresses can, however, be correlated in the same way as in the case of stress-free materials, indicating that the wealth of characterization formulas pertinent to indentation hardness is available also for the purpose of residual field determination. Only cone indentation of elastic-perfectly plastic materials is considered, but the generality of the results is discussed in some detail.

Keywords elastic deformations, hardness values, residual stresses, sharp indentation

1. Introduction

Residual stresses can be a very dangerous feature when it comes to reduction in load-carrying capacity and strength in general. Such stresses can of course be introduced through mechanical and/or thermal loading but also during engineering, processing and production of monolithic and composite materials. Naturally, the best way to avoid any destructive influence from residual stresses is to substantially reduce the levels of the residual fields. However, very often this is not an easy task to undertake, and then, a more realistic approach to the problem is to quantify these stresses and account for them during design and dimensioning. There are numerous methods that have been suggested for this purpose (hole-drilling, layer removal, beam bending, neutron and x-ray tilt techniques just to mention a few), but lately indentation testing has emerged as an easy and nondestructive alternative. Accordingly, residual stress determination using indentation has developed into a very active research field during the last decades.

Arguably, this research started in a systematic manner when Tsui et al. (Ref 1) and Bolshakov et al. (Ref 2) investigated, some twenty years ago, experimentally and numerically the influence of residual stress on indentation properties at indentation of aluminum alloy 8009, by experimental and numerical (finite element) methods. In short, fundamental results were presented, showing that indentation hardness, in this paper defined as the average contact pressure, was invariant of such stresses while the amount of piling-up of material at the

contact contour showed clear stress dependence. In short, piling-up increased at compression and decreased at tension. Further pertinent investigations include (Ref 3-12) (just to mention a few) introducing more theoretical approaches to the analysis of the mechanics of the problem. In most of these studies, progress was made based on the fact that hardness was not affected by residual stresses and the deformation at the contact contour could then be directly correlated with the magnitude of the residual (or applied stresses) present in the indented material.

Even though the invariance of indentation hardness obviously is a fundamental part, in an analysis of residual stress effects at indentation, the accuracy of this feature has not been investigated in great detail from a theoretical/numerical point of view. Scattered results have been presented in, for example, (Ref 2, 4) and also in more detail in (Ref 13). In the latter case, general residual (applied) surface stresses were considered. One important aspect of this is the influence on the invariance from elastic deformations. This is somewhat surprising as the few pertinent results that exist regarding this matter, cf. (Ref 12, 14), indicate that when elastic effects are noticeable, invariance is lost. This is not an issue for standard metallic materials, but could be so, for example, for polymers and ceramics where elastic deformations around the contact region are in the same order as the plastic ones. It is therefore the intention of the present paper to investigate this matter in some detail.

2. Theoretical Background

The theoretical foundation laid down in (Ref 4, 5, 12) will be relied upon for background. This foundation rests on the invariance of hardness which will be tested presently using the finite element method; in particular, the commercial package ABAQUS (Ref 15) is used.

The analyses concern cone indentation with an angle $\beta = 22^\circ$ (corresponding to the angle at Vickers indentation), see Fig. 1, of elastic-ideally plastic materials. Plasticity is

Per-Lennart Larsson, Department of Solid Mechanics, Royal Institute of Technology, 10044 Stockholm, Sweden. Contact e-mail: plla@kth.se.

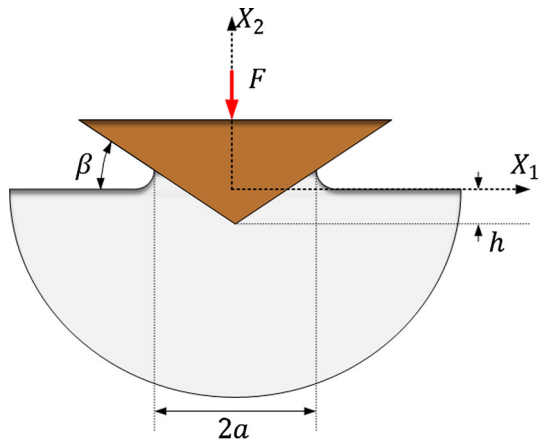


Fig. 1 Schematic of the geometry of the cone indentation test where a represents the true contact radius. In the present investigation, $\beta = 22^\circ$. The nominal contact area $A_{nom} = \pi h^2 / (\tan \beta)^2$ where h is the indentation depth

modeled using the standard Prandtl-Reuss (Mises) equations. Only homogeneous residual equi-biaxial stress fields are considered. The restrictions of the problem are introduced for clarity but not for necessity. The results will be correlated based on the well-known nondimensional strain parameter Λ suggested by Johnson (Ref 16, 17) according to

$$\Lambda = E \tan \beta / (\sigma_y (1 - \nu^2)) \quad (\text{Eq 1})$$

where E , ν and σ_y are Young's modulus, Poisson's ratio and the initial material flow stress, respectively. It should be noted that in Eq 1, only elastic-ideal plasticity is considered, but this limitation can be taken care of by replacing σ_y with the flow stress at a representative value of the effective plastic strain. Furthermore in (1), β is the angle between the sharp indenter and the undeformed surface of the material, as indicated in Fig. 1 for a cone indenter geometry. By using the Λ -parameter, Johnson (Ref 16, 17) also characterized three levels, see Fig. 2, of indentation (contact) behavior pertinent to the behavior of the material hardness H . These levels are: level I representing almost purely elastic indentation, level II representing a contact behavior where both elastic and plastic material properties are of importance and level III corresponding to a case where plasticity dominates the indentation problem (this level is at sharp indentation pertinent to most engineering metals and alloys).

Based on extensive investigations, cf., e.g., (Ref 4, 5), it is properly confirmed that the material hardness is invariant of residual stresses at level III contact. Other global indentation properties do, however, show dependence of such stresses and of particular interest; then, the relative contact area is

$$c^2 = A / A_{nom}. \quad (\text{Eq 2})$$

In (2), the areas A (true contact area) and A_{nom} (nominal contact area) are pertinent to projected contact areas, see Fig. 1. Note that $c^2 = 1$ when neither sinking-in nor piling-up occurs at the contact boundary.

This dependence was analyzed in (Ref 4, 5), and the formula

$$c^2 = c^2(\epsilon_{res}, \sigma_{res} = 0) - 0.32 \ln(1 + (\sigma_{res} / \sigma_y(\epsilon_{res}))) \quad (\text{Eq 3})$$

was derived for the case of equi-biaxial residual stresses σ_{res} and residual effective plastic strains ϵ_{res} . Other parameters in

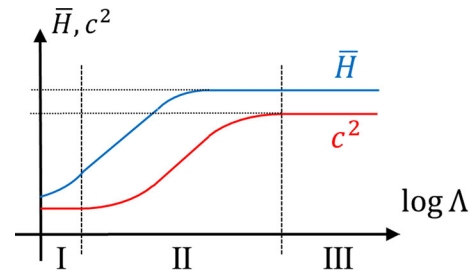


Fig. 2 Normalized hardness, $\bar{H} = H / \sigma_y$, and area ratio, c^2 , as functions of $\ln \Lambda$, Λ defined according to Eq 1. Schematic of the correlation of sharp indentation testing of elastic-ideally plastic materials. The three levels of indentation responses, I, II and III, are also indicated. Approximately, level II contact initiates at $\Lambda = 3$ level III contact at $\Lambda = 900$. The \bar{H} -curve flattens out at (approximately) $\Lambda = 30$

(3) are: $c^2(\epsilon_{res}, \sigma_{res} = 0)$ is the c^2 -value for a strained material with no residual stress and $\sigma_y(\epsilon_{res})$ is the yield stress of the material exhibiting a residual effective plastic strain ϵ_{res} . At ideal plasticity, Eq 3 becomes

$$c^2 = c^2(\sigma_{res} = 0) - 0.32 \ln(1 + (\sigma_{res} / \sigma_y)) \quad (\text{Eq 4})$$

due to the fact that the yield stress does not depend on the plastic strain state. It should be mentioned, as discussed in (Ref 11), that predictions made by Eq 3 and 4 are more accurate in tension than in compression.

The theoretical foundation for Eq 3 and 4 is the equivalence of mechanical fields close to the indenter in case of either contact-induced stresses in a virgin (unstressed) material or contact-induced stresses in a material with an initial material yield stress $\sigma_y + \sigma_{res}$. This was shown in (Ref 4, 5) from numerical (FEM) simulations. Accordingly, using an apparent yield stress

$$\sigma_{y,apparent} = \sigma_y + \sigma_{res} \quad (\text{Eq 5})$$

in Λ in Eq 1, according to

$$\Lambda = E \tan \beta / (\sigma_{y,apparent} (1 - \nu^2)), \quad (\text{Eq 6})$$

makes it possible to rely on the universal c^2 -curve in Fig. 2 regardless if residual stresses are present or not. As a consequence, the universal c^2 -curve in Fig. 2 can be used to determine σ_{res} in a situation where $c^2(\sigma_{res} = 0)$ is known. The accuracy of this approach to residual stress determination is of course based on the finding that elasticity influences c^2 in a wider range of Λ -values than what is the case for the hardness, see Fig. 2.

However, the above discussed difference of mechanical behavior at tension and compression reduced the accuracy of the results when relying on Eq 4. For this reason, Rydin and Larsson (Ref 12) restudied the definition of $\sigma_{y,apparent}$ and it was found that general high accuracy was achieved by replacing Eq 5 with the expression

$$\sigma_{y,apparent} = \sigma_y + F \sigma_{res}, \quad (\text{Eq 7})$$

where

$$\begin{aligned} F &= 0.52, \quad \sigma_{res} < 0 \\ F &= 1.77, \quad \sigma_{res} > 0. \end{aligned} \quad (\text{Eq 8})$$

Explicitly, it was suggested in (Ref 12) that the relation

$$c^2 = c^2(\sigma_{\text{res}} = 0) - 0.35 \ln(1 + (F\sigma_{\text{res}}/\sigma_y)) \quad (\text{Eq 9})$$

should replace Eq 4 above. Physically, this should be interpreted in the way that any deviation in indentation parameter values, from the corresponding values for the virgin material, is due to residual stress effects. It was shown by Rydin and Larsson (Ref 12) that Eq 9 improved very much on the situation as compared with the results from Eq 4. High accuracy predictions in both tension and compression were achieved as depicted in Fig. 3 where excellent agreement should be noted.

As mentioned repeatedly above, the usefulness of Eq 9 rests on the hardness invariance. Otherwise, the solution approach becomes much more complicated as, for example, ε_{res} in Eq 3 cannot be determined with any acceptable accuracy when strain-hardening effects are at issue. Even though invariance is firmly established, as discussed repeatedly above, there are also a few other studies, cf. (Ref 12, 14), indicating that when elastic effects are noticeable, invariance is lost. To clarify this matter is of considerable importance in this context and in particular then to correlate these findings with the Johnson (Ref 16, 17) parameter Λ . In doing so, the results by Rydin and Larsson (Ref 12) will be scrutinized, but also supplemented by presently performed finite element calculation to be described below.

3. Numerical Analysis

The numerical analysis rests on the finite element method. However, before discussing the discretization of the problem, the fundamental assumptions will be presented.

As stated repeatedly above, quasi-static cone indentation of elastic-ideally plastic prestressed materials is analyzed here. Relying upon classical elastoplasticity (Mises), this indicates that plastic deformations occur when

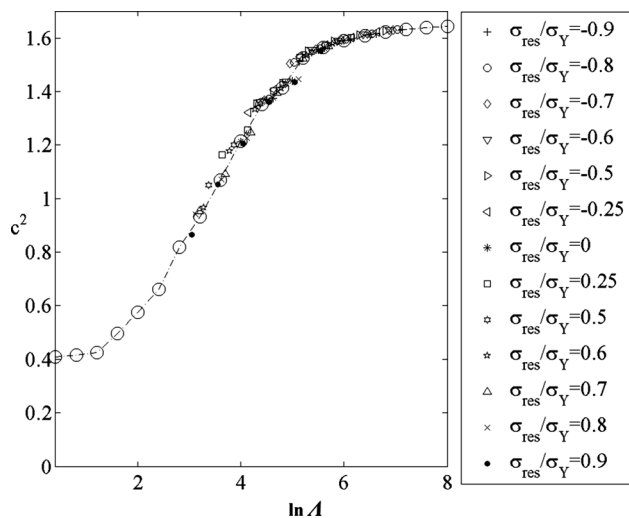


Fig. 3 Area ratio, c^2 , as function of $\ln \Lambda$, Λ defined according to Eq 6 with the yield stress σ_y replaced by the apparent yield stress $\sigma_{y,\text{apparent}}$ in Eq 7. Cone indentation of elastic-ideally plastic materials is considered. The results are taken from Rydin and Larsson (Ref 12)

$$\sigma_e = \sigma_y. \quad (\text{Eq 10})$$

The governing equations are formulated for large deformations (Ref 18), and accordingly, when the material is loaded elastically (or unloaded), the constitutive behavior is determined by Hooke's law formulated hypoelastically. Furthermore, frictionless contact is assumed in the finite element calculations as it has been shown by, for example, Giannakopoulos and Larsson (Ref 19) and Carlsson et al. (Ref 20), that friction will have a very small influence on hardness and relative contact area.

The discretization and finite element solution of the problem rests on the approach described in previous studies (Ref 19, 21-23). This procedure was further developed in (Ref 4, 5, 12) to also account for residual (applied) stresses. Accordingly, the foundation for the numerical analysis in the present paper is well established.

The finite element mesh used in the calculations is shown in Fig. 4. It goes almost without saying that axisymmetry is assumed. The entire mesh is shown in Fig. 4(a), and mesh details close to the indenter are shown in Fig. 4(b). In total, the mesh consists of 4567 four-noded axisymmetric hybrid elements and 4816 nodes. Hybrid elements were used in order to facilitate convergence at dominating plastic deformation.

In order to introduce residual (applied) stresses, into the finite element simulations, the movement of the outer boundary of the mesh was prescribed by radial displacements u prior to indentation, see Fig. 5. During the indentation process, u was kept constant. With such a prestress (pre-deformation), axisymmetry still holds and equi-biaxiality of applied stresses is ensured. It should be emphasized that the values on the radial displacements u are chosen in such a way that residual (applied) stresses are always in the elastic range.

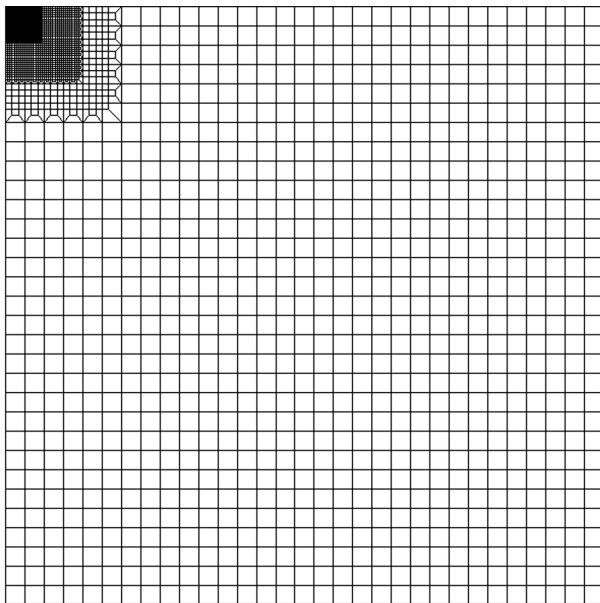
The resulting set of governing equations were solved using the commercial finite element program ABAQUS (Ref 15). With a numerical solution to the problem obtained, the material hardness was calculated from the indentation load F and the projected contact area A , according to

$$H = F/A. \quad (\text{Eq 11})$$

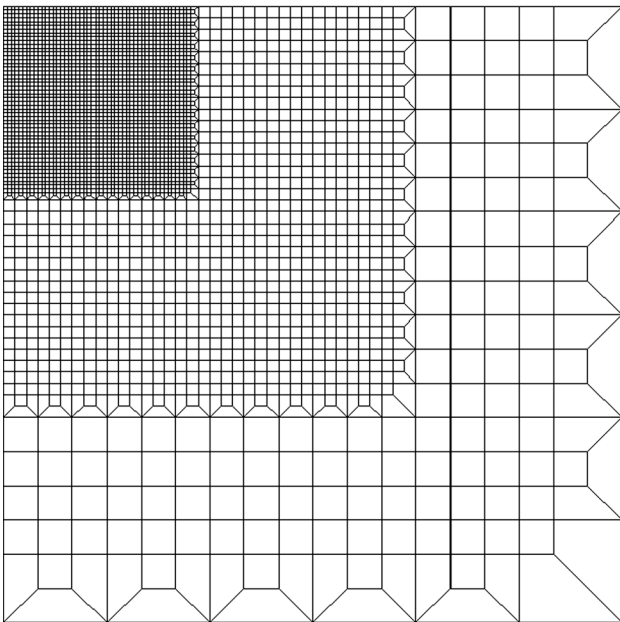
4. Results and Discussion

In the presentation below, the behavior of the material hardness at cone indentation of elastic-ideally plastic materials will be investigated in the presence of in-plane ($X_1 - X_3$ -plane) equi-biaxial residual (or applied) stresses. The investigation is based on the finite element method and the material properties, and the residual fields are described by the Johnson (Ref 16, 17) parameter Λ , in Eq 1 and 6, and the stress ratio $\sigma_{\text{res}}/\sigma_y$. The efforts are mainly devoted toward an understanding of the behavior of the hardness, Eq 10, at level II indentation when the influence from elasticity is substantial. At level III indentation, it is well known, as discussed in detail above, that the hardness is invariant of residual stresses.

It seems appropriate to first of all discuss some previous results directly relevant for this investigation. This concerns some results by Rydin and Larsson (Ref 12) where the hardness was determined for the cases $\ln \Lambda = 3, 5$ [Λ determined according to Eq 1 not accounting for the apparent yield stress in



(a)



(b)

Fig. 4 Finite element mesh used in the numerical calculations. (a) Complete mesh. (b) Details close to the region of contact

Eq 7] and for different values on the stress ratio σ_{res}/σ_y . A summary of the results by Rydin and Larsson (Ref 12) is shown in Fig. 6. Clearly, when $\ln \Lambda = 5$, the hardness in Fig. 6(a) is as stated many times above, independent of the residual stress state. However, when $\ln \Lambda = 3$, the hardness in Fig. 6(b) decreases substantially at tensile residual stresses. It should be noted that the horizontal line corresponds to the rigid-plastic (level III) solution determined by Atkins and Tabor (Ref 24) reading

$$H = 2.54\sigma_y \quad (\text{Eq 12})$$

at cone indentation and to be compared with the famous Tabor (Ref 25) relation

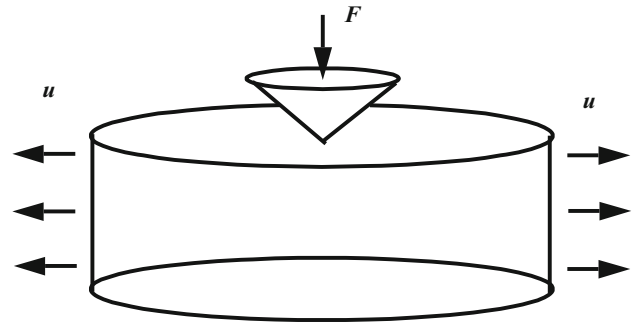


Fig. 5 Schematic of the pre-indentation loading. u is the prescribed radial displacement at the outer surface generating applied (residual) stresses

$$H = 2.8\sigma_y \quad (\text{Eq 13})$$

at rigid-plastic Vickers indentation.

With the results in Fig. 6 in mind, it is illustrative to scrutinize hardness results presented in the same way as shown in Fig. 3 for the area ratio c^2 depicted as function of the Johnson (Ref 16, 17) parameter Λ [defined according to Eq 1]. This is done in Fig. 7 clearly showing the three levels of indentation schematically shown in Fig. 2 but now based on actual finite element results. Figure 7 shows that $\ln \Lambda = 3$ constitutes an approximate border between level II and level III indentation. According to the results shown in Fig. 6(b), this transition occurs when $\ln \Lambda$ is slightly less than 3 when defining Λ according to Eq 6 with $\sigma_{y,apparent}$ according to Eq 7. Clearly, the results in Fig. 6 and 7 are in conformity and this will be further investigated in the spirit of the corresponding results for c^2 in Fig. 3 in the context of residual stresses.

Consequently, in Fig. 8 the results in Fig. 6 and 7 are combined with Λ defined by Eq 6 with $\sigma_{y,apparent}$ according to Eq 7. Obviously, the (normalized) hardness values H/σ_y fall on a single master curve, indicating that this parameter can be correlated with residual stresses in the same way as the area ratio c^2 .

From an analysis point of view, this is a remarkable finding as it indicates that all previously derived formulae, aiming at material characterization using indentation testing, can be applied also in case of residual stress determination by indentation. Indeed, this is so also at level II indentation where elastic effects are pronounced.

It should be admitted immediately that this conclusion rests on a few numerical results from Fig. 6. Accordingly, additional finite element calculations, as described above, were performed in order to confirm this finding. The materials investigated in this case were defined by

$$\ln \Lambda = 3.4, 3.52 \quad (\text{Eq 14})$$

with the Johnson (Ref 16, 17) parameter Λ defined according to Eq 1. These rather close values were chosen in order to secure that the stress-free material was pertinent to level III contact while the behavior entered the level II regime in the presence of tensile residual stresses. As regards residual stresses, the values

$$(\sigma_{res}/\sigma_y) = 0, 0.25, 0.375, 0.5, 0.75, 1.0 \quad (\text{Eq 15})$$

were chosen (not all combinations of the parameters in Eq 14 and 15 were investigated). Obviously, only tensile residual

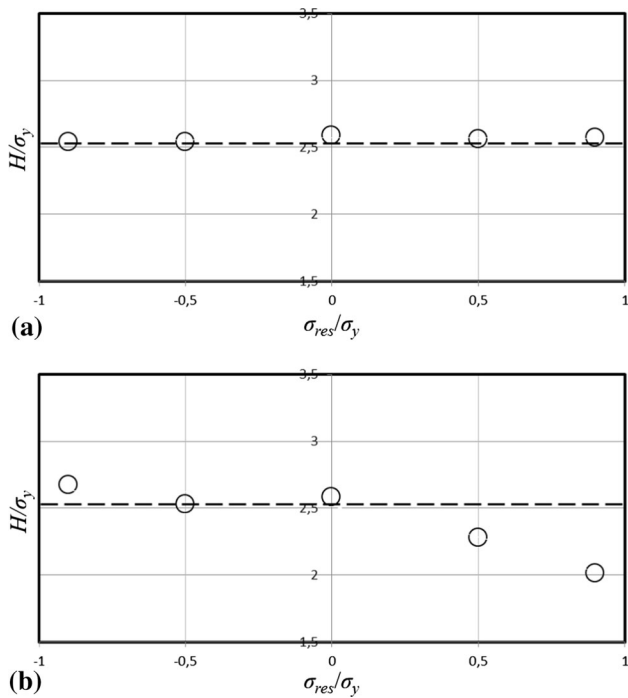


Fig. 6 Influence of residual stress on hardness values. Normalized hardness, H/σ_y , as function of residual stress ratio, σ_{res}/σ_y . Cone indentation of elastic-ideally plastic materials is considered. The straight line represents Eq 12. The results are taken from Rydin and Larsson (Ref 12). (a) $\ln \Lambda = 5$ where Λ is defined according to Eq 1. (b) $\ln \Lambda = 3$ where Λ is defined according to Eq 1

stresses are considered for the reason that compressive ones would increase Λ , when defined according to Eq 6 and 7, leading to a more pronounced level III (rigid-plastic) situation.

The present numerical results based on Eq 14 and 15 are introduced in Fig. 9 and 10, and again, these results indicate that also in this case $\ln \Lambda = 3$ constitutes an approximate border between level II and level III indentation and that the explicit hardness values fall right on the master curve defined by the stress-free hardness values in Fig. 7, see especially Fig. 10. The latter finding is true for both new level II and level III results.

Consequently, it can be stated that with Λ defined by Eq 6, with $\sigma_{y,apparent}$ according to Eq 7, both hardness and area ratio c^2 can be directly correlated with stress-free master curves for these quantities. This is indeed valid in the entire range of indentation values pertinent to different levels of indentation.

The present finding is indeed an encouraging one, when it comes to residual stress determination by sharp indentation, as it suggests that also the hardness value (and not only the area ratio c^2) can be used for such a purpose. As already mentioned above, this is especially attractive as it indicates that the wealth of characterization formulas pertinent to indentation hardness is available also for the purpose of residual field determination. It should be emphasized though this additional information is only available at level II indentation. At the level III indentation, the (normalized) hardness is independent of the Johnson (Ref 16, 17) parameter Λ , see Eq 12 and 13, and consequently invariant of residual stresses as discussed exten-

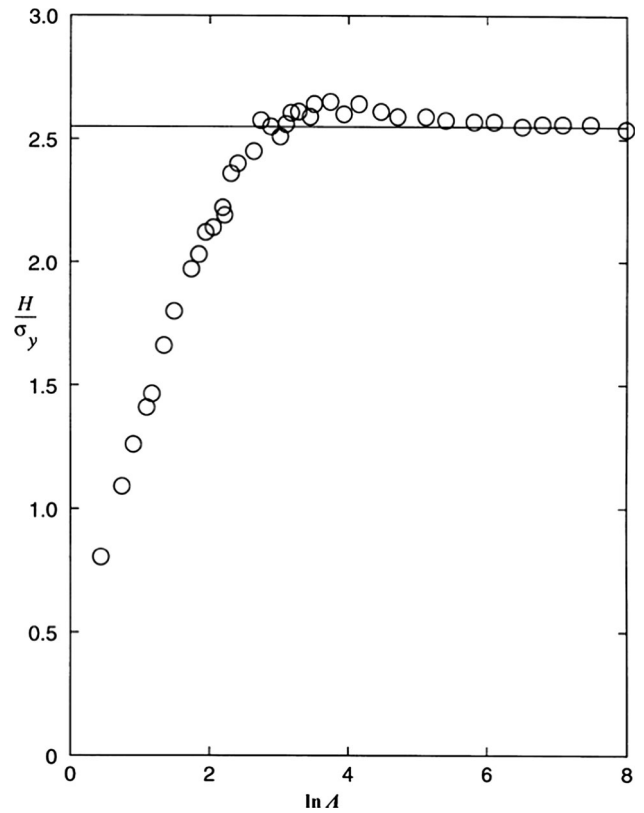


Fig. 7 Normalized hardness, H/σ_y , as function of $\ln \Lambda$, Λ defined according to Eq 1. Cone indentation of elastic-ideally plastic materials is considered. The straight line represents Eq 12. Stress-free results taken from Larsson (Ref 23)

sively and in detail above. This feature naturally also brings up the problem of demarcating between level II and level III indentation. An obvious partial remedy to this is of course to carefully characterize the virgin material and to determine where the corresponding Λ -value falls on the hardness curve in Fig. 7. In addition, adherence to Eq 12 (Ref or Eq 13) also indicates if level II or level III indentation is at issue. Also the value on the area ratio c^2 can give further information regarding this issue.

Obviously, the analysis above is restricted to cone indentation of elastic-ideally plastic materials with equi-biaxial residual stress fields. This is not a major issue though as an extension of the theoretical foundation to successfully include also plastic strain-hardening, general biaxial stresses as well as other indenter geometries have been extensively discussed in, for example, (Ref 5, 26). The practical details of this matter are left for future studies.

Finally, it is worth mentioning that the present approach could very well be applied to other types of contact problems. One of these problems could be scratching and scratch testing where correlation of material and contact properties, in the spirit of Johnson (Ref 16, 17), has been discussed for some time now, cf. (Ref 27-35). It remains, however, to undertake an analysis that incorporates also residual stresses in this special type of global quantity correlation.

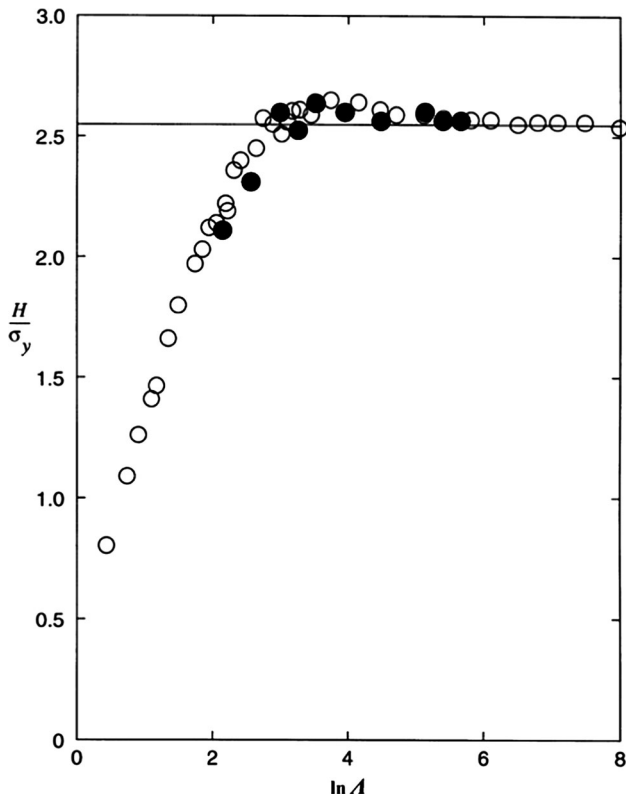


Fig. 8 Normalized hardness, H/σ_y , as function of $\ln\Lambda$, Λ defined according to Eq 6 with the yield stress σ_y , replaced by the apparent yield stress $\sigma_{y,\text{apparent}}$ in Eq 7. Cone indentation of elastic-ideally plastic materials is considered. The straight line represents Eq 12. Open circle, stress-free results taken from Larsson (Ref 23). Filled circle, the hardness values in Fig. 6 with and without residual stresses

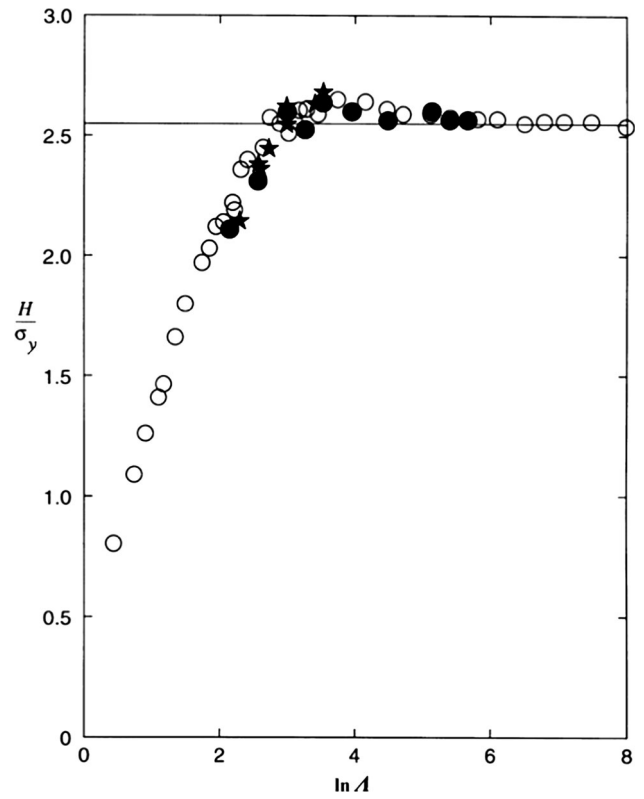


Fig. 10 Normalized hardness, H/σ_y , as function of $\ln\Lambda$, Λ defined according to Eq 6 with the yield stress σ_y , replaced by the apparent yield stress $\sigma_{y,\text{apparent}}$ in Eq 7. Cone indentation of elastic-ideally plastic materials is considered. The straight line represents Eq 12. Open circle, stress-free results taken from Larsson (Ref 23). Filled circle, the hardness values in Fig. 6 with and without residual stresses. Asterisk, the hardness values in Fig. 9 with and without residual stresses

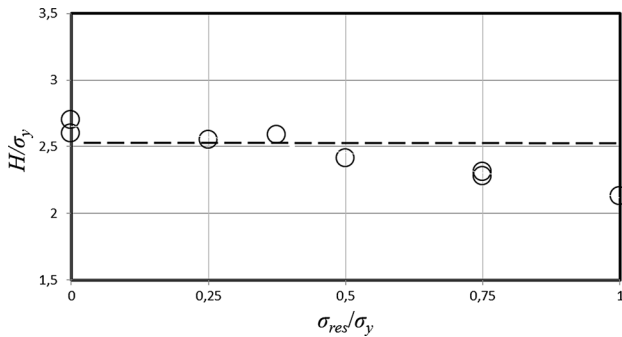


Fig. 9 Influence of residual stress on hardness values. Normalized hardness, H/σ_y , as function of residual stress ratio, $\sigma_{\text{res}}/\sigma_y$. Cone indentation of elastic-ideally plastic materials is considered. The straight line represents Eq 12. The present results for the material and residual stress state defined in Eq 14 and 15

5. Conclusions

Cone indentation of elastic-ideally plastic materials has been investigated numerically, using the finite element method, and theoretically. The most important findings can be summarized as follows:

- The global indentation properties, hardness and contact area ratio can be completely correlated using a single nondimensionalized strain parameter regardless if residual stresses are present in the material or not.
- This correlation is achieved by accounting for residual stress in the definition of the material yield stress.
- This result creates new possibilities of practical importance for residual stress determination by sharp indentation testing when elastic and plastic deformations induced by indentation are of equal magnitude as an abundance of formulas used for material characterization using indentation is available also when it comes to determination of residual stresses.
- At rigid-plastic indentation, i.e., negligible elastic deformations, the hardness is, as determined also in previous studies, invariant of residual stresses and only the contact area ratio is available for the determination of such mechanical fields.

The theoretical foundation necessary to incorporate also plastic strain-hardening, general biaxial stresses as well as other indenter geometries, has been laid down in previous studies, but the details pertinent to such an analysis specifically related to the present findings are left for future studies.

Open Access

This article is distributed under the terms of the Creative Commons Attribution 4.0 International License (<http://creativecommons.org/licenses/by/4.0/>), which permits unrestricted use, distribution, and reproduction in any medium, provided you give appropriate credit to the original author(s) and the source, provide a link to the Creative Commons license, and indicate if changes were made.

References

1. T.Y. Tsui, W.C. Oliver, and G.M. Pharr, Influences of Stress on the Measurement of Mechanical Properties Using Nanoindentation. Part I. Experimental Studies in an Aluminum Alloy, *J. Mater. Res.*, 1996, **11**, p 752–759
2. A. Bolshakov, W.C. Oliver, and G.M. Pharr, Influences of Stress on the Measurement of Mechanical Properties Using Nanoindentation. Part II. Finite Element Simulations, *J. Mater. Res.*, 1996, **11**, p 760–768
3. S. Suresh and A.E. Giannakopoulos, A New Method for Estimating Residual Stresses by Instrumented Sharp Indentation, *Acta Mater.*, 1998, **46**, p 5755–5767
4. S. Carlsson and P.L. Larsson, On the Determination of Residual Stress and Strain Fields by Sharp Indentation Testing. Part I. Theoretical and Numerical Analysis, *Acta Mater.*, 2001, **49**, p 2179–2191
5. S. Carlsson and P.L. Larsson, On the Determination of Residual Stress and Strain Fields by Sharp Indentation Testing. Part II. Experimental Investigation, *Acta Mater.*, 2001, **49**, p 2193–2203
6. J.G. Swadener, B. Taljat, and G.M. Pharr, Measurement of Residual Stress by Load and Depth Sensing Indentation with Spherical Indenters, *J. Mater. Res.*, 2001, **16**, p 2091–2102
7. Y.H. Lee and D. Kwon, Stress Measurement of SS400 Steel Beam Using the Continuous Indentation Technique, *Exp. Mech.*, 2004, **44**, p 55–61
8. Y.H. Lee and D. Kwon, Estimation of Biaxial Surface Stress by Instrumented Indentation with Sharp Indenters, *Acta Mater.*, 2004, **52**, p 1555–1563
9. M. Bocciarelli and G. Maier, Indentation and Imprint Mapping Method for Identification of Residual Stresses, *Comput. Mater. Sci.*, 2007, **39**, p 381–392
10. N. Huber and J. Heerens, On the Effect of a General Residual Stress State on Indentation and Hardness Testing, *Acta Mater.*, 2008, **56**, p 6205–6213
11. P.L. Larsson, On the Mechanical Behavior at Sharp Indentation of Materials with Compressive Residual Stresses, *Mater. Des.*, 2011, **32**, p 1427–1434
12. A. Rydin and P.L. Larsson, On the Correlation Between Residual Stresses and Global Indentation Quantities: Equi-Biaxial Stress Field, *Tribol. Lett.*, 2012, **47**, p 31–42
13. P.L. Larsson and P. Blanchard, On the Invariance of Hardness at Sharp Indentation of Materials with General Biaxial Residual Stress Fields, *Mater. Des.*, 2013, **52**, p 602–608
14. C.L. Eriksson, P.L. Larsson, and D.J. Rowcliffe, Strain-Hardening and Residual Stress Effects in Plastic Zones Around Indentations, *Mater. Sci. Eng., A*, 2003, **340**, p 193–203
15. ABAQUS. User's Manual Version 6.9. Pawtucket, RI: Hibbit, Karlsson and Sorensen Inc; 2009
16. K.L. Johnson, The Correlation of Indentation Experiments, *J. Mech. Phys. Solids*, 1970, **18**, p 115–126
17. K.L. Johnson, *Contact Mechanics*, Cambridge University Press, Cambridge, 1985
18. P.L. Larsson, Modelling of Sharp Indentation Experiments: Some Fundamental Issues, *Philos. Mag.*, 2006, **86**, p 5155–5177
19. A.E. Giannakopoulos and P.L. Larsson, Analysis of Pyramid Indentation of Pressure Sensitive Hard Metals and Ceramics, *Mech. Mater.*, 1997, **25**, p 1–35
20. S. Carlsson, S. Biwa, and P.L. Larsson, On Frictional Effects at Inelastic Contact Between Spherical Bodies, *Int. J. Mech. Sci.*, 2000, **42**, p 107–128
21. A.E. Giannakopoulos, P.L. Larsson, and R. Vestergaard, Analysis of Vickers Indentation, *Int. J. Solids Struct.*, 1994, **31**, p 2679–2708
22. P.L. Larsson, E. Söderlund, A.E. Giannakopoulos, D.J. Rowcliffe, and R. Vestergaard, Analysis of Berkovich Indentation, *Int. J. Solids Struct.*, 1996, **33**, p 221–248
23. P.L. Larsson, Investigation of Sharp Contact at Rigid Plastic Conditions, *Int. J. Mech. Sci.*, 2001, **43**, p 895–920
24. A.G. Atkins and D. Tabor, Plastic Indentation in Metals with Cones, *J. Mech. Phys. Solids*, 1965, **13**, p 149–164
25. D. Tabor, *Hardness of Metals*, Cambridge University Press, Cambridge, 1951
26. P.L. Larsson, On the Determination of Biaxial Residual Stress Fields from Global Indentation Quantities, *Tribol. Lett.*, 2014, **54**, p 89–97
27. J.L. Bucaille, E. Felder, and G. Hochstetter, Mechanical Analysis of the Scratch Test on Elastic and Perfectly Plastic Materials with Three-Dimensional Finite Element Modeling, *Wear*, 2001, **249**, p 422–432
28. J.L. Bucaille, E. Felder, and G. Hochstetter, Experimental and Three-Dimensional Finite Element Study of Scratch Test of Polymers at Large Deformations, *J. Tribol.*, 2004, **126**, p 372–379
29. E. Felder and J.L. Bucaille, Mechanical Analysis of the Scratching of Metals and Polymers with Conical Indenters at Moderate and Large Strains, *Tribol. Int.*, 2006, **39**, p 70–87
30. S. Bellemare, M. Dao, and S. Suresh, The Frictional Sliding Response of Elasto-Plastic Materials in Contact with a Conical Indenter, *Int. J. Solids Struct.*, 2007, **44**, p 1970–1989
31. F. Wredenberg and P.L. Larsson, On the Numerics and Correlation of Scratch Testing, *J. Mech. Mater. Struct.*, 2007, **2**, p 573–594
32. M. Ben Tkaya, M. Zidi, S. Mezlini, H. Zahouani, and P. Kapsa, Influence of the Attack Angle on the Scratch Testing of an Aluminium Alloy by Cones: Experimental and Numerical Studies, *Mater. Des.*, 2008, **29**, p 98–104
33. F. Wredenberg and P.L. Larsson, Scratch Testing of Metals and Polymers—Experiments and Numerics, *Wear*, 2009, **266**, p 76–83
34. N. Aleksey, G. Kermouche, A. Vautrin, and J.M. Bergheau, Numerical Study of Scratch Velocity Effect on Recovery of Viscoelastic-Viscoplastic Solids, *Int. J. Mech. Sci.*, 2010, **52**, p 455–463
35. S. Bellemare, M. Dao, and S. Suresh, A New Method for Evaluating the Plastic Properties of Materials Through Instrumented Frictional Sliding Tests, *Acta Mater.*, 2010, **58**, p 6385–6392